ACS Catalysis

RESEARCH ARTICLE

pubs.acs.org/acscatalysis

C−H versus O−H Bond Dissociation for Alcohols on a Rh(111) Surface: A Strong Assistance from Hydrogen Bonded Neighbors

Carine Michel,[†] Florian Auneau,[†,‡] Françoise Delbecq,[†] and Philippe Sautet*[,†]

[†]Université de Lyon, CNRS, Institut de Chimie de Lyon, Ecole Normale Supérieure de Lyon, 15 Parvis Descartes, BP7000, F-69342 Lyon Cedex 07, France

[‡]Université de Lyon, CNRS, Institut de Recherches sur la Catalyse et l'Environnement de Lyon IRCELYON, Université Lyon I, UMR5256, 2, avenue Albert Einstein, F-69626 Villeurbanne Cedex, France

ABSTRACT: Density functional theory (DFT) calculations show that hydrogen bonded neighbors can assist or hinder alcohol dehydrogenation on a metal catalyst. This critical role on C−H and O−H bond ruptures is addressed through two main cases: (i) the intermolecular hydrogen bond in the coadsorption of ethanol and water, and (ii) the intramolecular hydrogen bonds in glycerol. In the case of ethanol dehydrogenation, we show that the best catalyst is not bare Rh(111) but a surface with pre-adsorbed water or ethanol, the reactant ethanol being hydrogen bonded to the chemisorbed molecule, in a favorable configuration for O−H dissociation at the Rh surface. In addition, the intrinsic C−H/O−H reactivity is altered by hydrogen bonded neighbors. The O−H bond dissociation barrier is lowered by up to 0.25 eV. Conversely, the C−H bond scission is slightly inhibited (barrier increased by 0.1 eV maximum). As a result, O−H dissociation becomes favored. Glycerol reactivity is modulated by intramolecular H-bonds, with an additional constraint imposed by the carbon skeleton. Its reactivity is different from that of an isolated ethanol molecule, again with a preference for O−H cleavage.

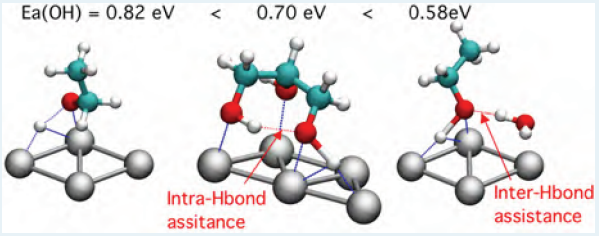

KEYWORDS: ethanol, glycerol, water, rhodium, DFT calculations, solvent effect, coadsorption effect, dehydrogenation

1. INTRODUCTION

Oxygenated products can be easily extracted from biomass. They have a 2-fold usefulness: they can be a potential source of CO_2 neutral energy[1−4] and they can be used as a sustainable raw material for the synthesis of complex and valuable chemicals.[5−10] For both applications, the dehydrogenation of alcohols is one of the central issues. It is a key reaction in the production of H_2 from bioalcohol.[11−13] It is also an essential step in the oxidation of alcohols into aldehydes and ketones, versatile intermediates for the synthesis of fine chemicals.[14−19] The dehydrogenation process requires the scission of C−H bonds and/or O−H bonds. In alkanes, the C−H bond scission is mainly catalyzed by supported metallic particles, the metal and the support being tailored depending on the desired products. For the C−H and O−H bond dissociation in alcohols, supported metallic particles are also used, but they have to be adapted not only to the presence of hydroxyl groups but also to the aqueous phase, the alcohols being generally solubilized in water.[20−22] This triggers important research efforts in the design of novel dehydrogenation catalysts in aqueous conditions.

To design new catalysts and new processes, a better insight in the fundamental aspects is required. Much is known currently on the catalysts' chemistry in the ultra high vacuum conditions, but this cannot be extrapolated to hydrated conditions. Indeed, water is a noninnocent solvent: the metal catalyst surface may be modified, the alcohol chemistry may be changed by the hydrogen bond network, and even more importantly, the solution pH is often a key parameter.

Theoretical studies have already proven to be an essential tool to accelerate the development of new catalysts by providing a better insight into the fundamental processes during a chemical transformation.[23−27] The adsorption and decomposition of isolated monoalcohols on a metallic slab have been investigated using the density functional theory (DFT) framework. For instance, the methanol decomposition on Pt(111) has been studied in detail at the DFT level by several groups,[28−34] this reaction being at the heart of the chemistry occurring at anodes of direct methanol fuel cells. Other metals have also been considered: Ni(111),[35] Pd(111),[36] Cu(110).[37] Another example is the numerous studies concerning the ethanol reactivity at metallic surfaces. They are motivated by the great number of applications, from ethanol reforming to produce H_2 to ethanol synthesis from syngas. Several surfaces have been considered: Pt(111),[38] Pd(111),[39,40] Rh(111)[41−43] and comparisons for several metallic surfaces.[44−46]

However, such theoretical studies are mostly limited to isolated monoalcohols interacting with the surface. Indeed, the influence of the environment is rarely addressed despite

Received: July 18, 2011
Revised: September 6, 2011
Published: September 07, 2011

its importance: solvent and/or coverage effects are seldom taken into account. The role of water on methanol oxidation at a Pt(111) surface has been scrutinized by Hartnig et al.:[31] the hydrogen bonded water molecule directly participates in the dehydrogenation reaction. Concerning the coverage effect, Yang et al.[41] have shown that ethanol tends to agglomerate into dimer on Rh(111), this process being driven by the intermolecular hydrogen bond between two ethanol molecules. Thus, intermolecular hydrogen bonds can deeply modify the chemistry of monoalcohols. Futhermore, polyols probably do not have the same chemistry than isolated monoalcohols: one can expect that intramolecular hydrogen bonds modify the reactivity of hydroxyl groups. However, such effects have been scarcely considered from a theoretical point of view up to now. We have recently compared the glycerol dehydration on three different surfaces, Ni(111), Rh(111), Pd(111), at a DFT level.[47] Glycerol is a simple-looking yet complicated polyol. It exhibits dozens of stable conformations in gas phase[48] and in water.[49−51] We have shown that the most stable chemisorbed structures of glycerol result from the balance between the metal−oxygen bonds and the intramolecular hydrogen bonds.[47]

In this Article, we want to probe how hydrogen bonds modulate the alcohol dehydrogenation process, either an intermolecular hydrogen bond with a neighboring molecule or a intramolecular hydrogen bond in a polyol. We base our study on previous results obtained on the Rh(111) surface by Yang et al.[41] The first step being generally the limiting step, we focus on the C−H and O−H bond activation in several cases. The isolated ethanol is our monoalcohol reference. Following Yang et al.,[41] we will consider the ethanol dimer and show how the C−H and O−H bond scission are modulated in presence of an additional ethanol molecule. Then, considering that most alcohols are solubilized in water, we will focus on the influence of a water molecule upon the ethanol reactivity. Finally, we will analyze the C−H and O−H bond dissociations in glycerol, the latter being a prototypical model of poly alcohols.

2. COMPUTATIONAL DETAILS

The calculations have been performed in the framework of Density Funtional Theory (DFT), using the Vienna Ab Initio Simulation Program (VASP).[52] The exchange-correlation energy and potential were calculated within the generalized gradient approximation (Perdew−Wang 91 functional).[53] A tight convergence of the plane-wave expansion was obtained with a cutoff of 400 eV. The electron-ion interactions were described by the projector augmented wave method (PAW) introduced by Blöchl[54] and adapted by Kresse and Joubert.[55]

The Rh(111) surface was modeled by a slab made of four layers separated by five layer-equivalents of vacuum. A 3 × 3 surface supercell was considered to model adsorption and reactions on the (111) surfaces. A Monkhorst-Pack mesh of 3 × 3 × 1 K points was used for the 2D Brillouin zone integration.[56] Adsorption and reaction processes were realized on the upper surface of the slab. The two bottom layers were kept fixed at the bulk-truncated positions (Rh−Rh interatomic distance 2.72 Å), while the coordinates of the two uppermost layers and of the adsorbates were relaxed until forces were less than 0.01 eV/Å.

The adsorption energy E_{ads} is calculated as the difference between the energy of the adsorption complex and that of the bare surface plus molecule in gas phase. A negative energy means a stabilizing adsorption. Upon molecular adsorption, the adsorbate and the surface will change their geometry. The adsorption energy can hence be decomposed in two terms: (i) the deformation energy E_{def}, always positive hence destabilizing, is the cost necessary to distort the surface and the molecule in the geometry of the chemisorbed system but keeping them separated; (ii) the interaction energy E_{int}, usually negative hence stabilizing, is the gain coming from the bond formation between the predeformed molecule and the surface in the chemisorption complex. Obviously, $E_{ads} = E_{def} + E_{int}$.

Reactions paths have been studied combining nudge elastic band procedures (NEB)[57,58] together with our local reaction path generator, OpenPath.[59] Transitions states have been optimized using the dimer method[60,61] and confirmed by the presence of a single imaginary vibration mode along the reaction coordinate.

We have focused on three main scissions in EtOH at Rh(111) surface: O−H, Cα−H, Cβ−H. Those simple catalytic processes have already been studied in the periodic DFT framework in the literature, but with contrasting results. Working on ethanol reforming on a large range of metals, among them Rh(111), Wang et al.[45] have found the C−H bond breaking at β position as being highly endothermic (+0.45 eV) with a low energy barrier (0.52 eV), lower than the activation energy of the O−H bond scission (0.58 eV). They do not even consider the C−H bond scission at the α position, claiming the energy barrier as being 1 eV higher.

Li et al.[43] have focused on the ethanol reactivity at the Rh(111) surface only. They provide both the Cα−H and Cβ−H dissociation barriers (1.75 and 1.33 eV respectively). According to their study, the O−H scission is even favored, with a much lower barrier (0.75 eV). The higher coverage (1/4 ML in the last study instead of 1/9 ML in Wang's study) cannot explain the large differences: working on ethanol synthesis from syngas, Choi et al[42] have a barrier of 0.71 eV for the Cα−H bond dissociation with a 1/4 ML coverage. Apparently, the starting ethanol configuration is crucial in the transition state search. There are two isoenergetic structures of ethanol adsorbed at the Rh(111), called cis- and trans- conformations by Li at al.[43] The one presented in Scheme 2 is the most stable at our level of calculation and corresponds to the cis-conformation in Li et al.'s paper.[43] The Cβ−H group is oriented toward the vacuum and consequently, the Cβ−H bond is poorly activated while the Cα−H bonds point toward the surface and can be easily activated by the metal catalyst. The other conformation (trans-conformation) is 0.03 eV higher in energy. The two Cα−H bonds are pointing up, not activated by the catalyst while the Cβ−H group is oriented toward the surface, the Cβ−H bond scission easily activated by the metallic catalyst. Li et al. and Wang et al. have both chosen to consider only the reaction of the trans-adsorbed ethanol, hence their higher energy barrier for Cα−H bond dissociation than the Cβ−H bond dissociation. Consequently, we have carefully tested various starting conformations for each transition state. In addition, we analyze in depth the evolution of the energy barriers depending on the considered molecules to go beyond the activation energies numbers.

3. RESULTS AND DISCUSSION

First, we report and discuss the comparative adsorption on Rh(111) of two alcohols: a monoalcohol, the ethanol (EtOH),

Scheme 1. Most Stable Structure for Two Ethanol Molecules Adsorbed at a Rh(111) Surface on the Left Hand Side and the Two Most Stable Structures for Glycerol Adsorbed at a Rh(111) Surface, *Gly1* and *Gly2*, in the Middle and in the Right Hand Side, Respectively[a]

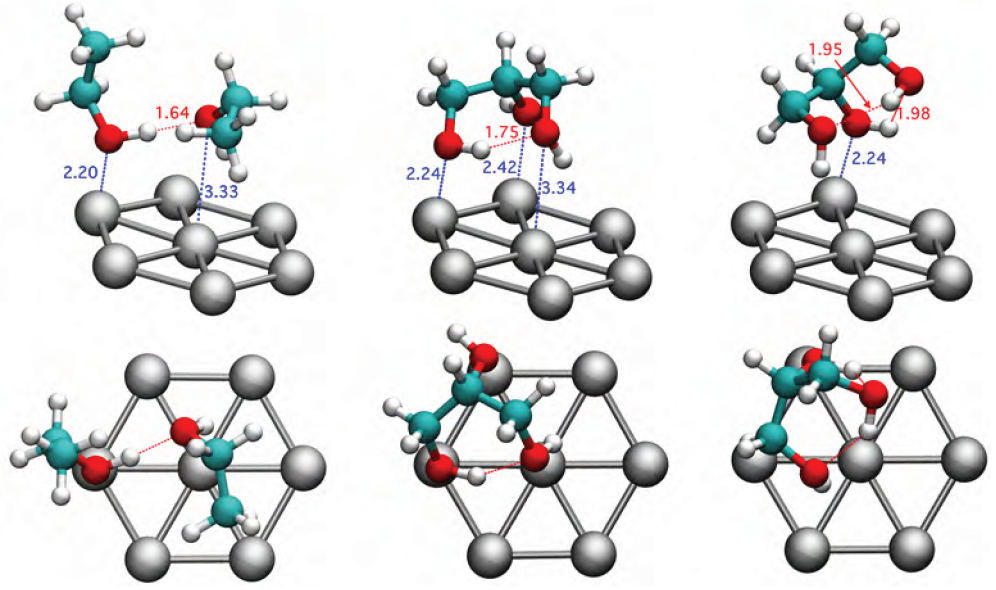

[a] Distances are indicated in Å.

Table 1. Alcohols Adsorption on a Rh(111) Surface[a]

alcohol	E_{ads} (eV)	d_{Rh-O} (Å)	d_{Hbond} (Å)	d_{Hbond} gas phase (Å)
EtOH	−0.46	2.25		
$(EtOH)_2$	−0.77	2.20/3.33	1.64	1.88
2 EtOH	−1.01	2.20/3.33	1.64	
Gly1	−0.60	2.24/2.42/3.34	1.76/	2.04/2.15
Gly2	−0.54	2.24/3.54	1.95/1.98	2.04/2.15

[a] Adsorption energies are given in eV. Distances are given in Å. For comparison, we report both the Hbond distances in the adsorbed geometry and in the gas phase geometry. When the alcohol considered is the ethanol dimer $(EtOH)_2$, the reference is the dimer in gas phase. When the alcohol considered is two ethanol molecules (2 EtOH), the reference is the two ethanol molecules isolated in gas phase.

Table 2. Energy Decomposition (in eV) of the Following Reaction: 2 EtOH + Rh → $(EtOH)_2$ @ Rh[a]

fragments	E_{int} (eV)
EtOH1 + EtOH2 → $(EtOH)_2$	−0.23
EtOH1 + Rh → EtOH1 @ Rh	−0.51
EtOH2 + Rh → EtOH2 @ Rh	−0.14
EtOH1 + EtOH2 + Rh → $(EtOH)_2$ @ Rh	−1.15

[a] The interaction energy E_{int} is the energy gain through the interaction between the fragments frozen in the optimal $(EtOH)_2$ @ Rh geometry. EtOH1 is the ethanol molecule closest to the rhodium surface, EtOH2 is the farther one.

and a polyol, the glycerol ($CH_2OH-CHOH-CH_2OH$). Then, we consider the O−H bond dissociation and the C−H bond dissociation in each case.

3.1. Adsorption. From our calculations, the isolated ethanol prefers to adsorb at a top site of Rh(111) binding to the surface through the oxygen atom. The calculated adsorption energies (−0.46 eV) and the main geometrical parameters are in agreement with previous studies on alcohols and water adsorption at a Rh(111) slab.[41−43,62,63] According to a previous theoretical study,[41] adsorbed ethanol molecules on Rh(111) agglomerate into hydrogen-bonded dimers. This is confirmed by our calculations. Indeed, an additional ethanol molecule is not adsorbed on the metallic surface (Rh−O = 3.33 Å) but preferentially interacts through a short hydrogen bond (O···H = 1.64 Å) with the initially adsorbed ethanol molecule (see Scheme 1): the O···H distance is 0.24 Å shorter than in the isolated dimer (see Table 1). In a H-bonded dimer, one can distinguished the H-bond donor, involved through its OH group and the H-bond acceptor, involved through an oxygen lone pair in the hydrogen bond. On Rh(111), the chemisorbed ethanol molecule is the donor while the additional ethanol molecule is the acceptor.

The formation of such a H-bond dimer, starting from one adsorbed and one gas phase ethanol molecule, leads to an energy gain of −0.55 eV. This is twice larger than the hydrogen bond energy gain (ca. −0.25 eV) for a gas phase dimer. Despite the long Rh−O distance (3.33 Å), this energy gain of 0.55 eV is also notably larger than the adsorption energy of the first ethanol molecule (−0.46 eV, Rh−O = 2.25 Å), see Table 1 and Scheme 1. To provide a better understanding of the situation, the interaction energy between the three partners is analyzed in more details in the geometry of the adsorbed dimer. The interaction energy between the three possible couples is reported in Table 2: −0.23 eV between the two ethanol molecules; −0.51 eV between the chemi-adsorbed ethanol molecule and the Rh(111) slab ; −0.14 eV between the distant ethanol molecule and the Rh(111) slab. The total sum of the two bodies interactions energy is −0.88 eV, to be compared with the three bodies interactions energy: −1.15 eV. The

dx.doi.org/10.1021/cs200370g |*ACS Catal.* 2011, 1, 1430–1440

Scheme 2. Structures of the Initial State, the Transition State, and the Final State along the O−H Bond Dissociation Pathway for (a) Ethanol, (b) Hydrogen Bond Acceptor Molecule of the Ethanol Dimer, (c) Ethanol Interacting with an Adsorbed Water Molecule, and (d) Water Interacting with an Adsorbed Ethanol Molecule[a]

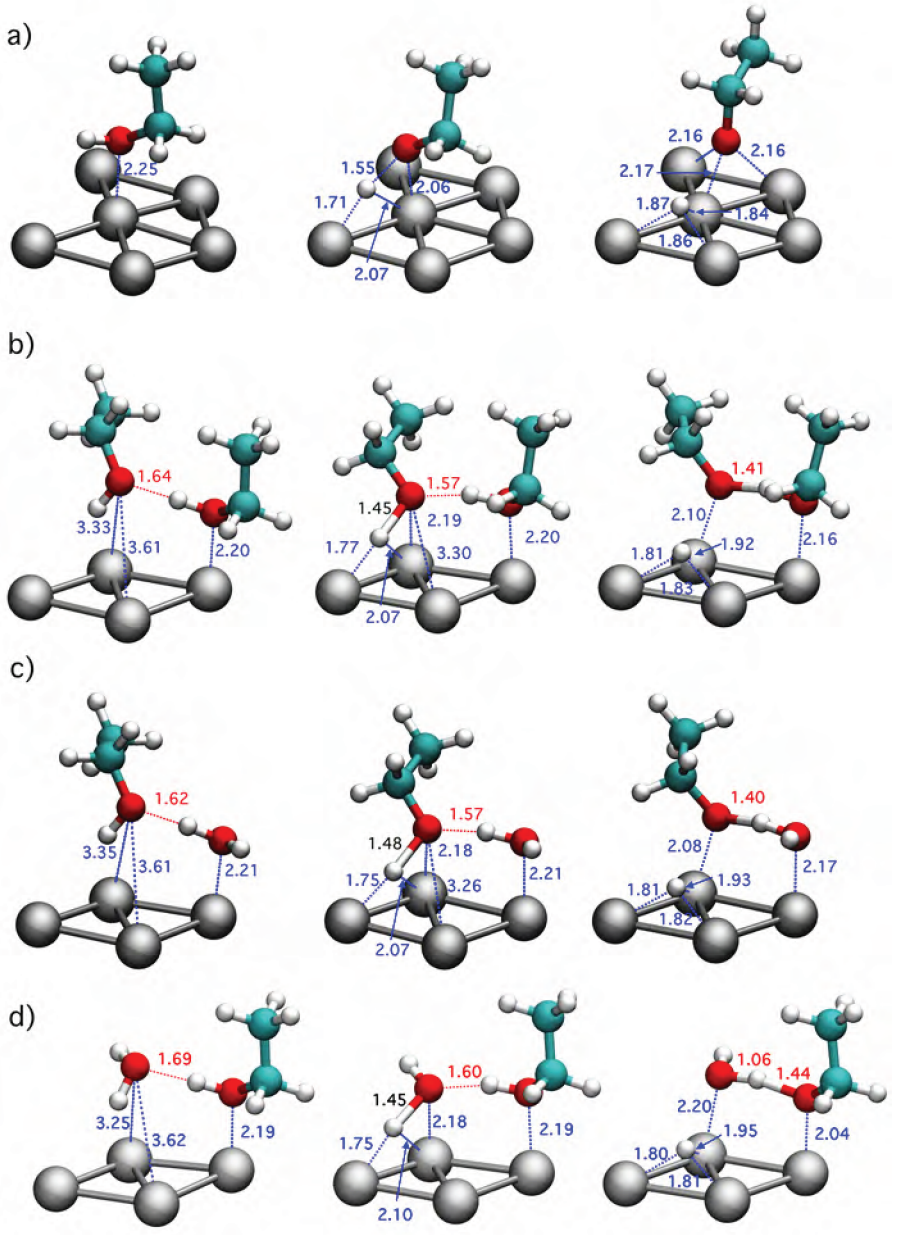

[a] Distances are indicated in Å.

difference is due to the synergy of this coadsorption: −0.27 eV. It is even stronger than the hydrogen bond (0.23 eV). Thus, it is probably the driving force favoring the formation of a hydrogen bond rather than the formation of a Rh−O bond during the addition of the second ethanol molecule. Another way to express this synergy is to compare the molecule-surface interaction energy for the dimer (−0.91 eV) with that for each ethanol molecule (0.51 and 0.14 eV in the geometry of the dimer). The mutual polarization of the two hydrogen bonded OH groups enhances both the hydrogen bond and the chemisorption on the surface.

The balance between the hydrogen bond formation and the Rh−O bond formation is even subtler in the case of glycerol adsorption. The glycerol is a C3 molecule with three hydroxyl groups, one on each carbon: two are at a terminal position; one is at the central position. In gas phase, glycerol can adopt several stable conformations including both five- and six-membered ring hydrogen bonds.[48] In the most stable one, the two terminal hydroxyls are hydrogen bonded forming a 6-membered ring cycle (O···H = 2.04 Å) and the central hydroxyl is hydrogen bonded to a terminal hydroxyl but weakly, forming a 5-membered ring cycle (O···H = 2.15 Å). We have already discussed the glycerol adsorption at a Rh(111) surface.[47] In the most stable configuration (*Gly1*), glycerol interacts with the metallic surface mainly through two oxygen atoms adsorbed on top sites (one terminal hydroxyl and the central hydroxyl) and the two terminal

dx.doi.org/10.1021/cs200370g |*ACS Catal.* 2011, 1, 1430–1440

Table 3. Energy of Reaction (ΔE, in eV), Activation Energy ($\Delta E^{\ddagger}$, in eV), and Main Distances (in Å) of the Transition State Structures for the O−H Bond Dissociation in Various Alcohols over a Rh(111) Surface[a]

reaction	ΔE	$\Delta E^{\ddagger}$	d_{O-H}	d_{Rh-O}	d_{Rh-H}
EtOH → Et−O + H	−0.19	0.82	1.55	2.06	2.07/1.71
EtOH−EtOH* → Et−O···HOEt + H	−0.09	0.57	1.45	2.19	2.07/1.77
EtOH−H_2O* → Et−O···H_2O + H	0.08	0.58	1.46	2.18	2.08/1.77
EtOH* − H_2O → Et−O···H2O + H	−0.13	0.64	1.46	2.18	2.10/1.75
Gly_1 → CH_2OH−CHOH−CH_2O + H	−0.03	0.70	1.41	2.24	2.00/1.83
Gly_2 → CH_2OH−CHOH−CH_2O + H	−0.09	0.80	1.43	2.17	2.00/1.80
Gly_1 → CH_2OH−CHO−CH_2OH + H	−0.29	0.67	1.47	2.11	2.20/1.72
Gly_2 → CH_2OH−CHO−CH_2OH + H	−0.33	0.99	1.54	2.09	2.12/1.70

[a] Here the products are considered at infinite distance from each other on the metallic surface. When a dimer is concerned, an asterisk * denotes the fragment closest to the metallic surface.

Scheme 3. Energy (in eV) along the O−H Bond Stretch (in Å) of Ethanol (Solid Line) and for the Acceptor Molecule of the Ethanol Dimer (Dashed Line) Isolated in Gas Phase

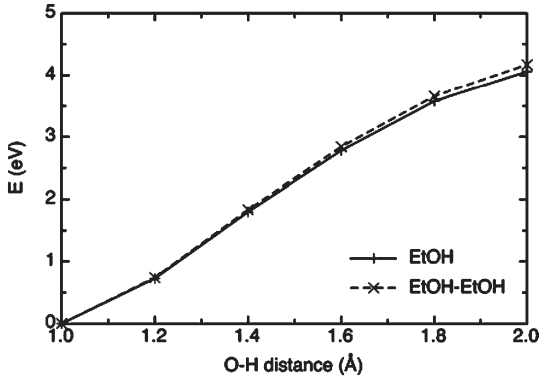

hydroxyls are still linked through a hydrogen bond forming a 6-membered ring (see the central structure in Scheme 1). The hydrogen bond between the central and the terminal hydroxyl is lost upon adsorption. As in the ethanol dimer, the hydrogen bond is considerably shortened upon adsorption (from 2.06 Å in gas phase to 1.76 Å in the adsorbed glycerol). The glycerol adsorption energy (−0.60 eV) is higher than the adsorption energy of ethanol (−0.46 eV) but lower than the adsorption energy of the ethanol dimer (−0.77 eV) (see Table 1)[64] since the position of the H-bonded O−H groups are constrained by the C_3 unit. If we try to keep as many hydrogen bonds as possible upon adsorption, we obtain the second lowest adsorption structure (*Gly2*), only 0.06 eV higher in energy, with one Rh−O bond (with a terminal hydroxyl) and keeping the two hydrogen bonds, one forming a 6-membered ring (1.95 Å) and the other one a 5-membered ring (1.98 Å) (see Scheme 1).

To conclude, the balance between hydrogen bond and metal−oxygen bond governs the adsorption process of alcohols. In absence of any additional constraint, the formation of hydrogen bond is more favorable than the formation of a Rh−O bond as we have seen in the case of the ethanol dimer. But any slight constraint can modify this intrinsic behavior. In the most stable conformation of glycerol in gas phase, the central-terminal H-bond is weak (O···H = 2.15 Å) because of the C3 skeleton strain. This explains why for glycerol, the formation of a Rh−O bond is slightly favored compared to the conservation of this intramolecular H-bond upon adsorption, as illustrated by the relative stability of the conformations *Gly1* and *Gly2*.

3.2. OH Dissociation. *3.2.1. Ethanol.* In an isolated ethanol adsorbed at Rh(111), the O−H bond dissociation is an exothermic process (−0.19 eV): the obtained ethoxy is strongly adsorbed at a ternary site (see Scheme 2). This scission holds an activation barrier of 0.82 eV. In the transition state structure, the O−H bond is stretched (1.55 Å), coplanar with Rh−Rh bond, the oxygen being on a top position and the hydrogen bridging the two rhodium atoms. The main distances are reported in Table 3. The initial, final, and transition state structures are reported in Scheme 2.

3.2.2. Ethanol Dimer. Let us now analyze how the O−H bond activation is modulated by a hydrogen bond in the ethanol dimer. First, one could imagine to dissociate the O−H bond of the donor molecule, bonded to the Rh surface, but the additional cost of the hydrogen bond breaking (0.23 eV) disfavors such a reaction. In revenge, the dissociation of the acceptor molecule is favorable despite the larger distance to the catalyst. Indeed, the O−H scission in the acceptor ethanol is almost athermic (−0.09 eV). The resulting ethoxy is adsorbed at a top site instead of the more stabilizing hollow site, stabilized by the ethanol donor through a strong hydrogen bond (1.41 Å). The presence of the ethanol donor has an even more striking effect on the dissociation barrier: it is 0.25 eV lower than in isolated ethanol (0.57 eV vs 0.82 eV). In addition, the transition state structure presents a similar but earlier structure (see Scheme 2): the stretched O−H bond is shorter (1.45 Å vs 1.57 Å), the Rh−O bond is longer (2.19 Å vs 2.06 Å), the hydrogen bond is shortened from 1.64 Å to 1.57 Å.[65] This earlier transition state with a lower barrier but with a less exothermic reaction may seem in contradiction with the Hammond postulate. In fact, the reaction energy given in Table 3 corresponds to the energy difference between the initial state (IS) and the final state (FS), where the two adsorbates are at infinite distance. When considering the energy difference between the initial state and the coadsorbed products (product state (PS)), the O−H scission in the ethanol monomer is more endothermic than in the ethanol dimer (+0.12 eV vs +0.05 eV, see Scheme 4, profiles (i) and (ii)), in agreement with the higher barrier (0.82 eV vs 0.57 eV).

Apparently, the ethanol O−H bond is activated when involved in a hydrogen bond as an acceptor. Is this activation intrinsic or is it specific to adsorbed molecules? Let us compare the O−H bond

dx.doi.org/10.1021/cs200370g |ACS Catal. 2011, 1, 1430–1440

Scheme 4. Energy Profile (in eV) along the O−H Bond Dissociation over a Rh(111) Surface in Three Cases: (i) in Black Solid Line, the Adsorbed Ethanol Monomer; (ii) in Red Solid Line, the Acceptor Molecule of the Adsorbed Ethanol Dimer; (iii) in Red Dashed Line, the Ethanol Monomer Frozen in the Geometry of the Acceptor Molecule of the Adsorbed Ethanol Dimer[a]

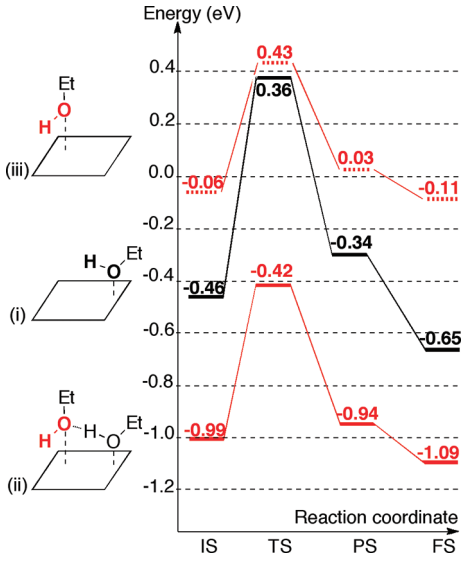

[a] The energy reference is the Rh(111) slab and two ethanol molecules at infinite distance. The initial state (IS) corresponds to the adsorption of one or two ethanol molecules. The transition state (TS) corresponds to the O−H bond dissociation. The product state (PS) corresponds to the co-adsorbed products. The final state (FS) corresponds to the two adsorbates at infinite distance from each other.

dissociation in ethanol and ethanol dimer in gas phase. The energy profile along the O−H bond distance in both cases is reported in Scheme 3. According to our results, stretching the O−H bond in the acceptor molecule of the gas phase dimer costs even more than in the ethanol monomer: the O−H bond is thus not weakened by the hydrogen bond. This raises the question of the H-bond role in the O−H bond scission.

In Scheme 4, we report the energy profile along the O−H bond dissociation path in the presence of the metallic surface in three cases: (i) the ethanol monomer, (ii) the ethanol dimer (O−H scission of the acceptor moiety), and (iii) the ethanol monomer frozen in the geometry of the acceptor ethanol of the dimer. This latter fictitious case does not represent a real pathway but is only used here to provide a better insight into the role of the hydrogen bond by removing the H-bond donor but keeping the imposed geometry for the acceptor. The energy difference between this fictitious profile (iii) and the ethanol monomer profile (i) quantifies the constraint imposed by the hydrogen bond. Conversely, the stabilization induced by this hydrogen bond is the energy difference between this fictitious profile (iii) and the dimer profile (ii).

We start the discussion analyzing the constraint imposed by the hydrogen bond on the dimer comparing the profiles (i) and (iii).[66] As we could expect, the adsorption energy of the isolated acceptor molecule is much weaker (−0.06 eV vs −0.46 eV) in agreement with the longer Rh−O distance (3.33 Å vs 2.25 Å). However, the transition state energy is almost the same for the ethanol monomer and the ethanol frozen in the acceptor geometry (0.07 eV difference, counting for the low constraint imposed by the H-bond). Thus, the energy barrier is much higher in the ethanol monomer (profile (i)) than in the ethanol monomer frozen in the acceptor geometry (profile (iii)): 0.82 eV vs 0.49 eV. An important difference lies also in the final state. As already discussed, the ethoxy is strongly stabilized at a ternary site of the Rh(111) surface, leading to an exothermic reaction energy (−0.19 eV, profile (i)). However in the ethanol acceptor path (profile (iii)), the ethoxy is adsorbed at a top site, in a configuration 0.60 eV higher in energy leading to a nearly athermic reaction energy (−0.05 eV). To conclude this comparison, the transition states are similar but the initial state and final state are destabilized in the ethanol acceptor geometry leading to a lower activation barrier and to an athermic reaction.

Now, let us focus on the stabilization provided by the hydrogen bond comparing the energy profile of the ethanol monomer frozen in the acceptor geometry (profile (iii)) with the one of the ethanol dimer (profile (ii)). The addition of the ethanol donor to the ethanol acceptor stabilizes the initial state, the transition state, and the final state by almost the same energy (ca. 0.90 eV), corresponding to the chemisorption, the H-bond formation, and the synergetic effect previously discussed. Thus, the low activation energy and the athermicity are kept upon the addition of the extra ethanol molecule.

To conclude, it should be pointed out that the O−H bond of the acceptor ethanol molecule is activated by the hydrogen bond through a geometrical effect, not an electronic effect. This hydrogen bond preorganizes the reactive ethanol molecule toward the Rh(111) surface inducing a preliminary partial desorption. The ethanol monomer is chemisorbed by the oxygen lone pair, a non bonding orbital, the H atom pointing up (see Scheme 2). This is not activating the O−H bond properly and the O−H bond must rotate to induce an overlap between the O−H bond pair and the Rh atom, in a triangular structure. Consequently, the molecule must decoordinate from the surface at the expense of the adsorption energy to reach a reactive configuration. On the contrary, in the case of the dimer, the reactive molecule is positioned in the right orientation for the O−H bond scission by its H-bonding interaction with the chemisorbed molecule. The H-bond is kept all along the O−H dissociation path and does not need to be broken, hence accompanying the reaction and allowing a reduced activation barrier. In a nutshell, the best catalyst is the Rh(111) surface with the ethanol donor adsorbed and not the bare Rh(111) surface.

3.2.3. Ethanol−Water Dimer. The role of the assistant hydrogen bond donor can also be played by a water molecule. The coadsorption of water and ethanol at a Rh(111) surface leads to two iso-energetic structures, structurally analogous to the ethanol dimer adsorption structure (see Scheme 2). Those two structures differ by the nature of the strongly adsorbed molecule, here indicated by an asterisk *. The coadsorption energy of a water molecule and an ethanol molecule on Rh(111) is similar to the coadsorption energy of two ethanol molecules (−1.03 eV and −1.01 eV respectively). The water can assist the ethanol O−H bond breaking in the first configuration H_2O^* −EtOH, playing the role of the hydrogen donor. As illustrated in Table 3 and Scheme 2, the water assistance is equivalent to the ethanol assistance: it lowers considerably the O−H scission barrier (from 0.82 to 0.58 eV) in a very similar way to the previous ethanol dimer. Surprisingly, the water can also assist the ethanol O−H bond breaking in the second configuration EtOH* $-H_2O$,

dx.doi.org/10.1021/cs200370g |ACS Catal. 2011, 1, 1430–1440

Scheme 5. Transition State Structures for the O−H Bond Dissociation in Glycerol[a]

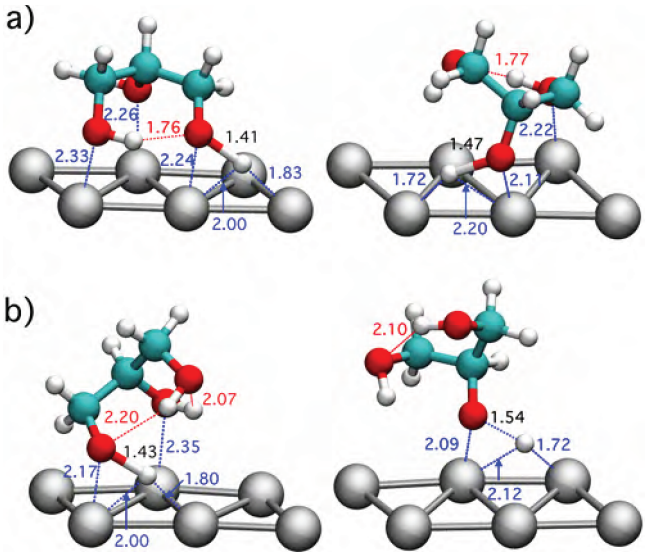

[a] Two reactive conformations are considered: (a) *Gly1*; (b) *Gly2*. The two positions, central and terminal, are reported: left panel, dissociation of the terminal O−H; right panel, the dissociation of the central O−H. Distances are indicated in Å.

playing the role of the hydrogen acceptor. In this configuration, the water is further from the surface, one of the two O−H bond pointing toward the rhodium surface. This water O−H bond is activated with a low barrier of scission (0.64 eV) leading to an adsorbed OH. Then, in the exit channel of the reaction, the ethanol hydroxyl hydrogen is transferred to the OH group, leading to the following final products: ethoxy radical, water, and hydrogen adsorbed on the Rh(111) surface. Thus, in both configurations, H_2O^* − EtOH and EtOH* − H_2O, the water assists the O−H dissociation in ethanol. This is a key result in alcohol oxidation at metal/water interface: preadsorbed water and first shell water can modify the adsorption mode of alcohols and play a substantial role in O−H bond activation.

3.2.4. Glycerol. Intermolecular hydrogen bonds substantially activate the O−H scission in ethanol. Thus, one may expect an autoactivation of O−H cleavage in polyols through intramolecular hydrogen bonds. However, the constraint imposed by the molecular skeleton may counterbalanced the preorganization by the hydrogen bond. We analyze now how those two effects influence the O−H bond rupture in glycerol.

In glycerol, the three hydroxyls are not equivalent, whatever the configuration considered (see Scheme 1). In the most stable configuration *Gly1*, the central hydroxyl is free of any hydrogen bond; the terminal hydroxyls are involved in a hydrogen bond, one playing the role of the donor, the other one of the acceptor. In the second most stable configuration *Gly2*, the central hydroxyl is strongly adsorbed at the Rh(111) surface, playing the role of a donor of hydrogen bond to a terminal hydroxyl; the terminal hydroxyls are not adsorbed, they are involved in a hydrogen bond, one playing the role of the donor, the other one of the acceptor.

For the O−H bond dissociation of a terminal hydroxyl, the situation is highly similar to the ethanol dimer case that we have just discussed: the O−H scission for the acceptor hydroxyl is comparable to the one of the acceptor ethanol. In the initial state *Gly1*, the acceptor hydroxyl group is far from the surface (Rh−O = 3.34 Å, see Scheme 1). The transition state structure is similar to all the previous O−H bond dissociations we have discussed (see Scheme 5).[67] The activation energy is a bit higher (see Table 3, $E^{\ddagger}$ = 0.70 eV) than in the ethanol dimer. This is related with the constraint imposed by the molecular skeleton. Indeed, the transition state structure must combine the activation of the terminal O−H bond with the adsorption of the two other hydroxyl groups. For similar reasons, in the final state, the oxygen atom is bonded to the surface through a top site (Rh−O = 2.05 Å), and the reaction is almost athermic (−0.09 eV) as in the ethanol dimer. We cannot perform the same decomposition analysis as in the ethanol dimer case, but the situation is highly analogous. We have also considered the O−H bond rupture in *Gly2*. The two terminal hydroxyls are here also hydrogen bonded, but none of them is adsorbed to the rhodium surface. The O−H scission of the acceptor hydroxyl is disfavored energetically: the obtained transition state is 0.15 eV higher in energy while the reaction is also athermic (0.03 eV). Here since the hydrogen bond donor is not adsorbed on the surface, the hydrogen bond cannot be conserved optimally along the reaction hence simply explaining the less favored pathway (the O−H bond is elongated to 2.20 Å in the transition state).

Let us now focus on the O−H scission at the central position. In the most stable conformation *Gly1*, the central hydroxyl is not involved in any hydrogen bond. Thus, one can expect high similarities between this hydroxyl dissociation and the one in isolated ethanol. Indeed, in the final state, the oxygen is also adsorbed at a ternary site and the reaction is exothermic (−0.29 eV). Here again, the transition state structure presents the same pattern. However the distances reveal an earlier transition state structure than in the isolated ethanol (O−H = 1.47 Å vs 1.57 Å) and the activation energy is much lower (0.67 eV vs 0.82 eV): surprisingly, the central O−H bond in *Gly1* has also a low activation barrier, even in absence of any hydrogen bond. In that case, the two terminal hydroxyls play also a fundamental role. Their presence prevails on the central hydroxyl to come close to the surface in the initial state (Rh−O = 2.42 Å). This is a key point in O−H bond activation as shown previously in the ethanol dimer case. Hence here a low barrier for O−H dissociation is also found, but the origin of the weak O−H/surface interaction is different. By contrast, in the glycerol conformation *Gly2*, the central hydroxyl is strongly adsorbed at the Rh(111) surface (Rh−O = 2.24 Å) and is hydrogen bonded as a donor to a terminal hydroxyl (O···H = 1.98 Å). Breaking the central O−H bond in this conformation is consequently much more expensive energetically ($\Delta E^{\ddagger}$ = 0.99 eV).

3.3. CH Dissociation. We discuss here how H-bonded neighbors can influence the C−H bond dissociation. Here again, we start with the isolated ethanol adsorbed on Rh(111) as a reference. Then, we focus on the influence of an extra water molecule upon the C−H cleavage in ethanol. Finally, we extend the discussion to the C−H dissociation in glycerol. The energy barriers, the reaction energies, and the main geometrical features of the transition states are reported in Table 4.

3.3.1. Ethanol. In ethanol, two different C−H bonds can be considered depending on the relative position to the hydroxyl, the Cα−H bond and the Cβ−H bond; however, they are analogous. In both cases, the C−H bond scission is an athermic process: ΔE (Cα−H) = −0.05 eV and ΔE (Cβ−H) = 0.04 eV. In addition, the energy barriers are almost the same (∼0.7 eV).

dx.doi.org/10.1021/cs200370g |*ACS Catal.* 2011, 1, 1430–1440

Table 4. Energy of Reaction (in eV), Activation Energy (in eV), and Main Distances (in Å) of the Transition State Structures for the C−H Bond Dissociation in Various Alcohols over a Rh(111) Surface[a]

reaction	ΔE	$\Delta E^{\ddagger}$	d_{C-H}	d_{Rh-C}	d_{Rh-H}
EtOH → $CH_3-CH-OH$ + H	−0.05	0.71	1.52	2.28	1.65
EtOH → CH_2-CH_2-OH + H	0.04	0.69	1.53	2.24	1.65
$EtOH-H_2O^*$ → $CH_3-CH-OH\cdots H_2O^*$ + H	0.12	0.83	1.52	2.29	1.67
$EtOH-H_2O^*$ → $CH_2-CH_2-OH\cdots H_2O^*$ + H	0.19	0.81	1.55	2.26	1.66
$EtOH^* - H_2O$ → $CH_3-CH-OH\cdots H_2O$ + H	−0.03	0.76	1.53	2.26	1.65
$EtOH^* - H_2O$ → $CH_2-CH_2-OH\cdots H_2O$ + H	0.08	0.70	1.53	2.24	1.66
Gly_1 → $CH_2OH-CHOH-CHOH$ + H	−0.08	0.80	1.52	2.27	1.66
Gly_2 → $CH_2OH-CHOH-CHOH$ + H	−0.19	0.72	1.48	2.31	1.62

[a] Here the products are considered at infinite distance from each other on the metallic surface. When a dimer is concerned, an asterisk * denotes the fragment closest to the metallic surface.

Scheme 6. Transition State Structures for the C−H Bond Dissociation in EtOH in α Position (Left Column) and β Position (Right Column) in Three Cases: (a) Isolated Ethanol, (b) Ethanol Assisted by an Adsorbed Water Molecule $EtOH-H_2O^*$, and (c) Adsorbed Ethanol Interacting with a Water Molecule $EtOH^* - H_2O$[a]

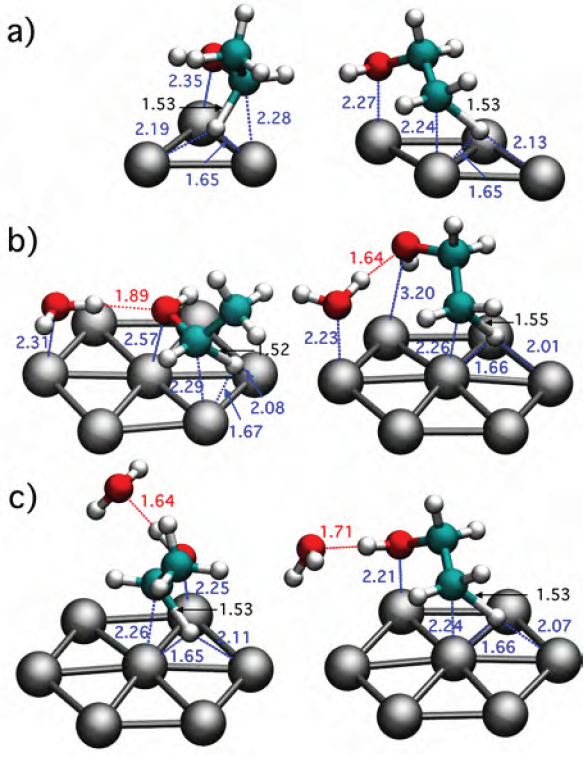

[a] Distances are indicated in Å.

Both transition state structures have a similar pattern (see Scheme 6): the oxygen atom is still sitting atop a Rh atom (Rh−O = 2.27−2.35 Å); the Rh/C/H atoms form a triangle (Rh−H ∼ 1.65 Å; Rh−C ∼ 2.25 Å; C−H ∼ 1.52 Å).[68]

This metal/C/H triangular pattern is common for C−H activation of alkanes on transition metal surfaces. For instance, the ethane molecule shows a slightly lower C−H dissociation barrier (0.62 eV) and a later transition state (Rh−H = 1.65 Å, Rh−C = 2.24 Å and C−H = 1.58 Å) than in ethanol. In ethanol, the chemisorption by the O atom induces a constraint interfering with the necessary molecular deformation to reach the optimal transition state, hence yielding to a higher dissociation barrier. This can be easily quantified by replacing the hydroxyl group by a hydrogen atom in the transition state structure of the Cα−H cleavage in EtOH: the resulting constrained structure is 0.17 eV higher than the optimal transition state for ethane. However, the relative position to the oxygen does not influence much the C−H bond breaking and the C−H scission is favored compared to the O−H dissociation in isolated ethanol adsorbed on a Rh(111) slab.

3.3.2. Ethanol−Water Dimer. As seen previously, the coadsorption of water and ethanol at a Rh(111) surface leads to two isoenergetic structures, differing by the nature of the strongly adsorbed molecule: H_2O^* −EtOH and $EtOH^*$ $-H_2O$. For each structure, the two possible C−H have been considered (in α and β position). The four corresponding transition state structures are reported in Scheme 6 (b and c). Compared to isolated adsorbed ethanol, the nature of the transition state is unchanged, mainly represented by a C/H/Rh triangle with the same typical distances (C−H = 1.52−1.55 Å ; Rh−C = 2.24−2.29 Å ; Rh−H = 1.65−1.67 Å). The activation energies, the reaction energies, and the main geometrical features of the transition states are reported in the Table 4 together with those of the isolated ethanol discussed above.

It is striking that the additional water molecule has a different impact on the ethanol C−H cleavage depending on its role: hydrogen bond donor or acceptor. Indeed, as a hydrogen bond acceptor in $EtOH^*$ $-H_2O$ (see Scheme 6, c), the added water molecule has almost no influence on the C−H scission process whereas it hinders this dissociation once adsorbed on the surface in H_2O^* −EtOH. Indeed, in this latter case, the dissociation process is endothermic (up to ΔE = 0.2 eV) and the energy barriers are increased (by 0.12 eV), in agreement with the Hammond postulate.

To quantify the balance between the stabilizing H-bond and the destabilizing carbon skeleton distortion, we propose to use the same analysis than in the previous paragraph on the OH scission. We report in Schemes 7 and 8 the activation steps for both Cα−H and Cβ−H scissions in three cases: (i) the ethanol monomer, (ii) the EtOH-H_2O dimer, and (iii) the ethanol monomer frozen in the dimer geometry. We have restricted the analysis to the initial state (IS) and the transition states (TS).

dx.doi.org/10.1021/cs200370g |ACS Catal. 2011, 1, 1430–1440

Scheme 7. Activation Step (in eV) along the C−H Bond Dissociation in the EtOH−H_2O* Dimer over a Rh(111) Surface in Three Cases: (i) in Black Solid Line, the Adsorbed Ethanol Monomer; (ii) in Red Solid Line, the Dimer; (iii) in Red Dashed Line, the Ethanol Monomer Frozen in the Geometry of the Dimer Geometry[a]

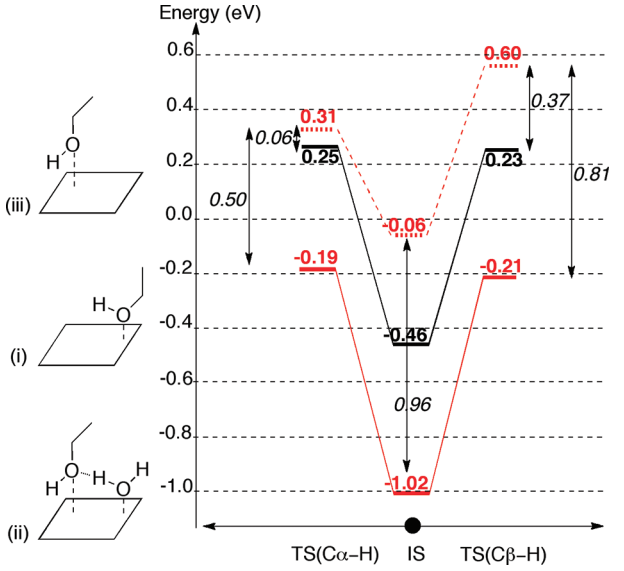

[a] The energy reference is the Rh(111) slab, an ethanol molecule, and a water molecule at infinite distance. The initial state (IS) corresponds to the adsorption of one ethanol molecule and in the dimer case, of a water molecule. The transition state (TS) corresponds to the C−H bond dissociation: in α position on the right, in β position on the left.

Scheme 8. Activation Step (in eV) along the C−H Bond Dissociation in the EtOH*−H_2O Dimer over a Rh(111) Surface in Three Cases: (i) in Black Solid Line, the Adsorbed Ethanol Monomer; (ii) in Red Solid Line, the Dimer; (iii) in Red Dashed Line, the Ethanol Monomer Frozen in the Geometry of the Dimer Geometry[a]

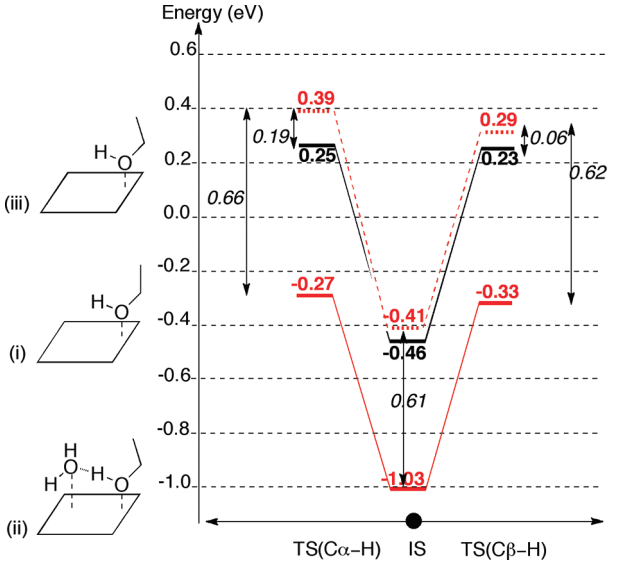

[a] The energy reference is the Rh(111) slab, an ethanol molecule, and a water molecule at infinite distance. The initial state (IS) corresponds to the adsorption of one ethanol molecule and in the dimer case, of a water molecule. The transition state (TS) corresponds to the C−H bond dissociation: in α position on the right, in β position on the left.

The energy difference between the TS of the ethanol monomer (profile (i)) and the TS of the ethanol monomer frozen in the dimer geometry (profile (iii)) quantifies the constrained imposed in the TS by the hydrogen bond and the nonideal character of the TS geometry compared to isolated ethanol. The energy difference between profile (iii) and (ii) corresponds to the stabilization induced by the water coadsorption through a hydrogen bond.

• *EtOH-H_2O* Dimer.* The corresponding profiles are reported in Scheme 7.

In α position, the water molecule interacts only weakly with the transition state: the energy gain when adding water is the smallest we observed (0.50 eV), in adequacy to the long H-bond in the transition state structure (1.89 Å, see Scheme 6, b). The Cα−H dissociation is here not compatible with the conservation of the H-bond with water. This weak interaction induces a weak distortion in the TS (0.06 eV). Thus, the higher barrier in the EtOH−H_2O* dimer (0.83 eV) than in the ethanol (0.71 eV) lies in the weakening of the hydrogen bond during the bond rupture.

In β position, the water molecule has a large effect in the C−H bond dissociation. The corresponding transition state is strongly distorted, the Rh−O interaction is almost lost (0.37 eV between profile (i) and (iii), Rh−O = 2.27 Å in the monomer and Rh−O = 3.20 Å in the dimer, see Scheme 6, a and b). Despite the partial compensation by the water coadsorption (energy gain of 0.81 eV in the transition state), this leads to a higher activation barrier in EtOH−H_2O* than in the monomer (0.81 and 0.69 eV respectively).

Scheme 9. Transition State Structures for the Terminal C−H Bond Dissociation in Glycerol[a]

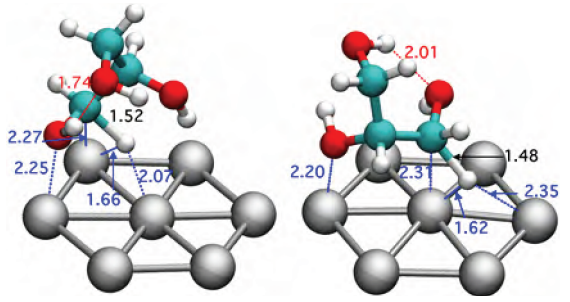

[a] Two reactive conformations are considered: left panel, *Gly1* ; right panel, *Gly2*. Distances are indicated in Å.

To conclude, the presence of the chemisorbed water molecule amplifies the constraint induced by the hydroxyl group on the C−H scission. It is indeed difficult to established the C−H dissociation transition state and at the same time to maintain the H-bond with the adsorbed water.

• *EtOH* −H_2O Dimer.* When the ethanol is kept adsorbed on the surface, the situation is different. The profiles are reported in Scheme 8 for this case. The water coadsorption has the same effect in the Cβ−H scission transition state than in the initial state: the stabilization is maintained (0.62 eV) and the slight distortion is comparable (0.06 eV against 0.05 eV). Hence the

dx.doi.org/10.1021/cs200370g |*ACS Catal.* 2011, 1, 1430–1440

energy barrier is conserved upon water coadsorption in this case. In the Cα−H scission transition state, the water coadsorption modifies slightly the activation energy (0.76 eV in EtOH* −H_2O vs 0.71 eV in EtOH): the greater stabilization in the transition state (0.66 eV) is compensated by the greater distortion (0.19 eV).

3.3.3. Glycerol. We examine next the C−H dissociation in glycerol, considering only the terminal position. Indeed, the dissociation of the C−H in central position requires a different reactive conformation: the central C−H bond is directed upward in the two most stable conformations we consider here, forbidding the activation by the catalyst. The dissociation of the C−H bond in the terminal position is feasible starting from both conformations we have considered here: *Gly1* and *Gly2*. The corresponding transition state structures are reported in Scheme 9. The starting conformation does not influence much the transition state energy (0.03 eV difference) nor the transition state structure, exhibiting here again the typical C/H/Rh triangle of the C−H bond scission. The energy barriers are in the same range than for the formally isolated ethanol and water−ethanol dimers: 0.70−0.80 eV. The *Gly1* C−H scission transition state is similar to the case of the H-bond donor ethanol with water (Scheme 6, c, left) while *Gly2* resembles the Cβ−H scission for adsorbed ethanol (Scheme 6, a, right).

4. CONCLUSION

The adsorption and reactivity of monoalcohols such as ethanol at metallic surfaces has generally been simulated in the literature in the absence of coadsorption effects. Coadsorbates can however strongly affect and assist the reactivity. In this Article, we demonstrate that the coadsorption of an additional ethanol molecule or a water molecule influences the ethanol adsorption at a Rh(111) surface and the subsequent C−H and O−H bonds activation. We also show that the same underlying mechanism triggers the catalytic reactivity of poly alcohols such as a glycerol.

On Rh(111), the coadsorption of two R−OH molecules (R═H or Et) results in a hydrogen bonded dimer, the hydrogen bond donor being in direct interaction with the metallic surface through a Rh−O bond while the hydrogen bond acceptor is farther, in weak interaction with the surface. In this chemisorbed dimer, the O−H bond scission is surprisingly facilitated in the weakly adsorbed hydrogen bond acceptor unit, while the C−H bond dissociation is slightly inhibited.

Consequently, the intrinsic O−H versus C−H selectivity can be reversed by the environment: for ethanol, the O−H bond scission becomes easier than the C−H in the presence of another ethanol molecule or an additional water molecule. The weak adsorption of the hydrogen bond acceptor is a key feature to explain the lowering of O−H bond scission. The strong constraint on the carbon skeleton imposed by the optimization of the H-bond interaction is in contrast at the origin of the inhibition of the C−H scission in EtOH in the presence of a H-bonded water molecule or a ethanol neighbor. Thus, wet surfaces and water/metal interfaces cannot be modeled by a vacuum/metal interface when considering alcohol dehydrogenation. The explicit description of at least one solvent molecule is necessary. These results also suggest that water can efficiently assist alcohol dehydrogenation in experimental conditions. This may explain the promotion effect of water on the catalytic activity for alcohol oxidation.[69−71]

Hydrogen bonds are essential when considering alcohol/water coadsorption and reactivity toward a metallic catalyst. They are also crucial in polyol catalytic transformation, such complex molecules being rich in intramolecular H-bonds. However, they are commonly modeled by simpler alcohols such as ethanol. We have shown here how the adsorption and the reactivity of glycerol is modulated by intramolecular hydrogen bonds. Its reactivity is intermediate between that of isolated ethanol and of ethanol coadsorbed with water. Here again the O−H bond scission is facilitated by the presence of other hydroxyl groups through the skeleton preconditioning and by an initial weak interaction with the surface and is hence easier to perform than the C−H bond scission. Consequently, the isolated ethanol cannot be a good model for glycerol. The general character of these conclusions on different transition metals remains however to be demonstrated.

The C−O and C−C bond ruptures are also essential steps in alcohol valorization. An influence of hydrogen bond neighbors on those processes can also be expected when catalyzed by rhodium based catalysts. The concept of assistance by a coadsorbate can as well be extended to other catalytic reactions, promoters and poisons, being special well-known cases.

AUTHOR INFORMATION

Corresponding Author

*E-mail: philippe.sautet@ens-lyon.fr.

Funding Sources

F.A. thanks the Ministère de la Recherche for financial support.

ACKNOWLEDGMENT

Ab initio calculations were performed using the local HPC resources of PSMN at ENS-Lyon and of GENCI (CINES/IDRIS), project x2010075609.

REFERENCES

(1) Huber, G. W.; Iborra, S.; Corma, A. *Chem. Rev.* **2006**, *106*, 4044–4098, PMID: 16967928.
(2) Navarro, R. M.; Pena, M. A.; Fierro, J. L. G. *Chem. Rev.* **2007**, *107*, 3952–3991.
(3) Kunkes, E. L.; Simonetti, D. A.; West, R. M.; Serrano-Ruiz, J. C.; Gartner, C. A.; Dumesic, J. A. *Science* **2008**, *322*, 417–421.
(4) Simonetti, D. A.; Dumesic, J. A. *Catal. Rev.* **2009**, *51*, 441–484.
(5) Corma, A.; Iborra, S.; Velty, A. *Chem. Rev.* **2007**, *107*, 2411–2502.
(6) Gallezot, P. *Catal. Today* **2007**, *121*, 76–91.
(7) Gallezot, P. *Green Chem.* **2007**, *9*, 295–302.
(8) Gallezot, P. *ChemSusChem* **2008**, *1*, 734–737.
(9) Corma, A.; Renz, M.; Susarte, M. *Top. Catal.* **2009**, *52*, 1182–1189.
(10) Gallezot, P. *Top. Catal.* **2010**, *53*, 1209–1213.
(11) Haryanto, A.; Fernando, S.; Murali, N.; Adhikari, S. *Energy Fuels* **2005**, *19*, 2098–2106.
(12) Vaidya, P.; Rodrigues, A. *Chem. Eng. J.* **2006**, *117*, 39–49.
(13) Ni, M.; Leung, d. Y. C.; Leung, M. K. H. *Int. J. Hydrogen Energy* **2007**, *32*, 3238–3247.
(14) Chheda, J. N.; Huber, G. W.; Dumesic, J. A. *Angew. Chem., Int. Ed.* **2007**, *46*, 7164–7183.
(15) Davda, R. R.; Shabaker, J. W.; Huber, G. W.; Cortright, R. D.; Dumesic, J. A. *Appl. Catal., B* **2005**, *56*, 171–186.
(16) Zheng, Y.; Chen, X.; Shen, Y. *Chem. Rev.* **2008**, *108*, 5253–5277.
(17) Behr, A.; Eilting, J.; Irawadi, K.; Leschinski, J.; Lindner, F. *Green Chem.* **2008**, *10*, 13–30.

(18) Corma, A.; Huber, G. W.; Sauvanauda, L.; O'Connor, P. *J. Catal.* **2008**, *257*, 163–171.
(19) Tong, X. L.; Ma, Y.; Li, Y. D. *Appl. Catal., A* **2010**, *385*, 1–13.
(20) van den Tillaart, J.; Kuster, B.; Marin, G. *Appl. Catal., A* **1994**, *120*, 127–145.
(21) Chaminand, J.; Djakovitch, L.; Gallezot, P.; Marion, P.; Pinel, C.; Rosier, C. *Green Chem.* **2004**, *6*, 359–361.
(22) Soares, R. R.; Simonetti, D. A.; Dumesic, J. A. *Angew. Chem., Int. Ed.* **2006**, *45*, 3982–3985.
(23) Neurock, M. *J. Catal.* **2003**, *216*, 73–88.
(24) Norskov, J. K.; Bligaard, T.; Hvolbaek, B.; Abild-Pedersen, F.; Chorkendorff, I.; Christensen, C. H. *Chem. Soc. Rev.* **2008**, *37*, 2163–2171.
(25) Norskov, J. K.; Bligaard, T.; Kleis, J. *Science* **2009**, *324*, 1655–1656.
(26) Norskov, J. K.; Bligaard, T.; Rossmeisl, J.; Christensen, C. H. *Nat. Chem.* **2009**, *1*, 37–46.
(27) Neurock, M. *Ind. Eng. Chem. Res.* **2010**, *49*, 10183–10199.
(28) Desai, S. K.; Neurock, M.; Kourtakis, K. *J. Phys. Chem. B* **2002**, *106*, 2559–2568.
(29) Greeley, J.; Mavrikakis, M. *J. Am. Chem. Soc.* **2002**, *124*, 7193–7201.
(30) Greeley, J.; Mavrikakis, M. *J. Am. Chem. Soc.* **2004**, *126*, 3910–3919.
(31) Hartnig, C.; Spohr, E. *Chem. Phys.* **2005**, *319*, 185–191.
(32) Cao, D.; Lu, G.-Q.; Wieckowski, A.; Wasileski, S. A.; Neurock, M. *J. Phys. Chem. B* **2005**, *109*, 11622–11633.
(33) Kandoi, S.; Greeley, J.; Sanchez-Castillo, M. A.; Evans, S. T.; Gokhale, A. A.; Dumesic, J. A.; Mavrikakis, M. *Top. Catal.* **2006**, *37*, 17–28.
(34) Niu, C.-Y.; Jiao, J.; Xing, B.; Wang, G.-C.; Bu, X.-H. *J. Comput. Chem.* **2010**, *31*, 2023–2037.
(35) Wang, G.-C.; Zhou, Y.-H.; Morikawa, Y.; Nakamura, J.; Cai, Z.-S.; Zhao, X.-Z. *J. Phys. Chem. B* **2005**, *109*, 12431–12442.
(36) Jiang, R.; Guo, W.; Li, M.; Fu, D.; Shan, H. *J. Phys. Chem. C* **2009**, *113*, 4188–4197.
(37) Mei, D.; Xu, L.; Henkelman, G. *J. Phys. Chem. C* **2009**, *113*, 4522–4537.
(38) Wang, H.-F.; Liu, Z.-P. *J. Am. Chem. Soc.* **2008**, *130*, 10996–11004.
(39) Wang, E. D.; Xu, J. B.; Zhao, T. S. *J. Phys. Chem. C* **2010**, *114*, 10489–10497.
(40) Li, M.; Guo, W.; Jiang, R.; Zhao, L.; Shan, H. *Langmuir* **2010**, *26*, 1879–1888, PMID: 20000800.
(41) Yang, M.-M.; Bao, X.-H.; Li, W.-X. *J. Phys. Chem. C* **2007**, *111*, 7403–7410.
(42) Choi, Y.; Liu, P. *J. Am. Chem. Soc.* **2009**, *131*, 13054–13061.
(43) Li, M.; Guo, W.; Jiang, R.; Zhao, L.; Lu, X.; Zhu, H.; Fu, D.; Shan, H. *J. Phys. Chem. C* **2010**, *114*, 21493–21503.
(44) Ferrin, P.; Simonetti, D.; Kandoi, S.; Kunkes, E.; Dumesic, J. A.; Norskov, J. K.; Mavrikakis, M. *J. Am. Chem. Soc.* **2009**, *131*, 5809–5815.
(45) Wang, J.-H.; Lee, C. S.; Lin, M. C. *J. Phys. Chem. C* **2009**, *113*, 6681–6688.
(46) Radilla, J.; Boronat, M.; Corma, A.; Illas, F. *Theor. Chem. Acc.* **2010**, *126*, 223–229.
(47) Coll, D.; Delbecq, F.; Aray, Y.; Sautet, P. *Phys. Chem. Chem. Phys.* **2011**, *13*, 1448–1456.
(48) Chelli, R.; Gervasio, F. L.; Gellini, C.; Procacci, P.; Cardini, G.; Schettino, V. *J. Phys. Chem. A* **2000**, *104*, 11220–11222.
(49) Chelli, R.; Gervasio, F. L.; Gellini, C.; Procacci, P.; Cardini, G.; Schettino, V. *J. Phys. Chem. A* **2000**, *104*, 5351–5357.
(50) Callam, C. S.; Singer, S. J.; Lowary, T. L.; Hadad, C. M. *J. Am. Chem. Soc.* **2001**, *123*, 11743–11754.
(51) Dashnau, J. L.; Nucci, N. V.; Sharp, K. A.; Vanderkooi, J. M. *J. Phys. Chem. B* **2006**, *110*, 13670–13677.
(52) Kresse, G.; Hafner, J. *Phys. Rev. B* **1993**, *47*, 558–561.
(53) Perdew, J. P.; Wang, Y. *Phys. Rev. B* **1992**, *45*, 13244–13249.
(54) Blöchl, P. E. *Phys. Rev. B* **1994**, *50*, 17953–17979.
(55) Kresse, G.; Joubert, D. *Phys. Rev. B* **1999**, *59*, 1758–1775.
(56) Monkhorst, H. J.; Pack, J. D. *Phys. Rev. B* **1976**, *13*, 5188–5192.
(57) Henkelman, G.; Uberuaga, B. P.; Jonsson, H. *J. Chem. Phys.* **2000**, *113*, 9901–9904.
(58) Sheppard, D.; Terrell, R.; Henkelman, G. *J. Chem. Phys.* **2008**, *128*, 134106.
(59) Fleurat-Lessard, P.; Dayal, P.,A chemist view on reaction path determination, to be published. Available at http://perso.ens-lyon.fr/paul.fleurat-lessard/ReactionPath.html.
(60) Henkelman, G.; Jonsson, H. *J. Chem. Phys.* **1999**, *111*, 7010–7022.
(61) Kastner, J.; Sherwood, P. *J. Chem. Phys.* **2008**, *128*, 014106.
(62) Carrasco, J.; Michaelides, A.; Scheffler, M. *J. Chem. Phys.* **2009**, *130*, 184707.
(63) Pozzo, M.; Carlini, G.; Rosei, R.; Alfè, D. *J. Chem. Phys.* **2007**, *126*, 164706.
(64) The adsorption energy of the ethanol dimer is the energy difference between the energy of adsorbed ethanol dimer and the energy of the free metallic slab plus the energy of the ethanol dimer in the gas phase.
(65) In this transition state, the hydrogen bond is parallel to another Rh−Rh bond at a 120° angle. When the hydrogen bond is parallel to a Rh−Rh bond at a 60° angle, the O−H scission barrier is 0.05 eV larger.
(66) One should note that the profile (iii) is fictitious; thus, the structure designed by TS is not a real transition state. We use it as a shortcut for "the ethanol monomer frozen in the acceptor ethanol molecule geometry in the transition state structure of the dimer".
(67) The O−H bond is stretched (1.41 Å), H pointing down, the O−H bond coplanar with a Rh−Rh bond, the oxygen in a top position (Rh−O = 2.24 Å) and the hydrogen bridging the two rhodium atoms (Rh−H = 2.00 Å; 1.83 Å). The only noticeable differences are the earlier nature of the transition state with a shorter O−H bond (1.41 Å) and the relative orientation of the hydrogen bond and the stretched O−H bond: they form a 120° angle in the ethanol dimer and a 180° angle in glycerol.
(68) Besides, there is a slight difference in the transition state structures depending on the carbon (α or β). The O−C bond is parallel to a Rh−Rh bond and the C−H bond is parallel to an adjacent Rh−Rh bond: upon Cα−H dissociation, the two Rh−Rh bonds are at a 60° angle while upon Cβ−H scission, the two Rh−Rh bonds form a 120° angle.
(69) Yang, X.; Wang, X.; Liang, C.; Su, W.; Wang, C.; Feng, Z.; Li, C.; Qiu, J. *Catal. Commun.* **2008**, *9*, 2278–2281.
(70) Yang, X.; Wang, X.; Qiu, J. *Appl. Catal., A* **2010**, *382*, 131–137.
(71) Frassoldati, A.; Pinel, C.; Besson, M. *Catal. Today* **2011**, doi:10.1016/j.cattod.2011.02.058.